Composite Right/Left-Handed Substrate Integrated Waveguide and Half Mode Substrate Integrated Waveguide Leaky-Wave Structures

Yuandan Dong, *Student Member, IEEE*, and Tatsuo Itoh, *Life Fellow, IEEE*

***Abstract*—Composite right/left-handed (CRLH) substrate integrated waveguide (SIW) and half mode substrate integrated waveguide (HMSIW) leaky-wave structures for antenna applications are proposed and investigated. Their propagation properties and radiation characteristics are studied extensively. Their backfire-to-endfire beam-steering capabilities through frequency scanning are demonstrated and discussed. These metamaterial radiating structures are realized by etching interdigital slots on the waveguide surface and the ground. The slot behaves as a series capacitor as well as a radiator leading to a CRLH leaky-wave application. Four antennas are fabricated, measured, and analyzed, including two balanced CRLH SIW designs characterized by single-side or double-side radiation, and two unbalanced HMSIW designs characterized by different boundary conditions. Antenna parameters such as return loss, radiation patterns, gain, and efficiency are all provided. Measured results are consistent with the simulation. All these proposed antennas possess the advantages of low profile, low cost, and low weight, while they are also showing their own unique features, like high directivity, quasi-omnidirectional radiation, miniaturized size, continuous beam-steering capabilities covering both the backward and forward quadrants, etc., providing much design flexibility for the real applications.**

***Index Terms*—Composite right/left-handed (CRLH), half mode substrate integrated waveguide (HMSIW), leaky-wave antennas, substrate integrated waveguide (SIW).**

I. Introduction

SUBSTRATE integrated waveguide (SIW) and half mode substrate integrated waveguide (HMSIW) have been very popular types of planar guided-wave structures over the past decade [1]–[5]. They are synthesized on a planar substrate with linear periodic arrays of metallic vias. They have desirable features such as low profile, low cost, and easy integration with planar circuits while maintaining the advantageous characteristics of conventional rectangular waveguide. They have enabled numerous applications on high-performance planar components [6]–[13]. The concepts of HMSIW and folded substrate integrated waveguide (FSIW) were proposed aiming at a further reduction of the transverse size of the SIW [4], [5]. And their propagation properties have been studied systematically in [14], [15].

Manuscript received March 02, 2010; revised July 27, 2010; accepted October 12, 2010. Date of publication December 30, 2010; date of current version March 02, 2011.

The authors are with the Electrical Engineering Department, University of California at Los Angeles, Los Angeles, CA 90095 USA (e-mail: yddong@ee.ucla.edu; itoh@ee.ucla.edu).

Color versions of one or more of the figures in this paper are available online at http://ieeexplore.ieee.org.

Digital Object Identifier 10.1109/TAP.2010.2103025

Metamaterials are defined as effectively homogeneous structures with unusual properties, which have been under extensive investigation recently [16]–[18]. Metamaterial-based transmission lines (TLs) possess some unique features such as backward-wave and infinite wavelength propagation. Several types of composite right/left-handed (CRLH) TL metamaterials using SIW have been proposed and studied in [19]–[22].

Based on the preliminary study shown in [23], this paper presents an extensive investigation of a family of CRLH SIW and HMSIW leaky-wave structures. Four types of leaky-wave antennas are implemented and analyzed using the proposed planar waveguide structures. Up to now various CRLH leaky-wave antennas based on different technologies have already been investigated and presented [24]–[29]. They all exhibit the backward-to-forward beam-steering capability through frequency scanning. It is also noted that the conventional SIW and HMSIW leaky-wave antennas are introduced and discussed in [30], [31], which achieve edge-radiation by increasing the period length between the vias or taking advantage of the open boundary of the HMSIW. In [32], a transverse slot array antenna fed by an HMSIW is proposed and developed. A novel SIW leaky-wave antenna with CRLH behavior is also demonstrated and discussed in [33], which requires a multi-layer PCB process and is rather complicated to realize.

Compared with the designs in the previous literature, the antennas developed in this paper are able to offer a backfire-to-endfire beam-scanning performance as well as an extremely easy way for implementation. They are achieved simply by etching interdigital slots on the top metal surface and the ground of the waveguide. The slot acts like a series capacitor, which, along with the waveguide inherent shunt inductor provided by the vias, creates the necessary condition to support the backward-wave radiation. Miniaturization can be achieved by making the antennas operated below the waveguide cutoff as well as adopting a half mode structure or a modified HMSIW configuration which will be shown later.

This paper is organized as follows. The geometry of the proposed leaky-wave structures is illustrated in Section II, where four types of CRLH SIW and HMSIW unit cells are introduced. Section III gives a discussion on the equivalent circuit and the dispersion properties of the unit cells. Sections IV and V present their applications to CRLH SIW and HMSIW leaky-wave antennas. Four types of antennas are analyzed, constructed and measured, which exhibit various features such as balanced or unbalanced operating schemes, quasi-omnidirectional radiation patterns, and miniaturized size while keeping a high gain. Their

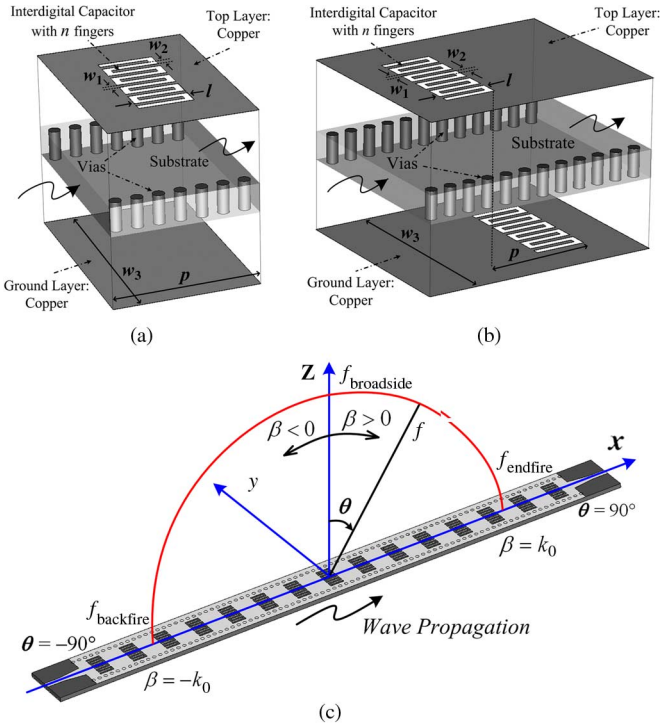

Fig. 1. Configuration of the proposed CRLH SIW leaky-wave structures (a) single-side radiating element, (b) double-side radiating element, and (c) overall SIW leaky-wave antenna prototype.

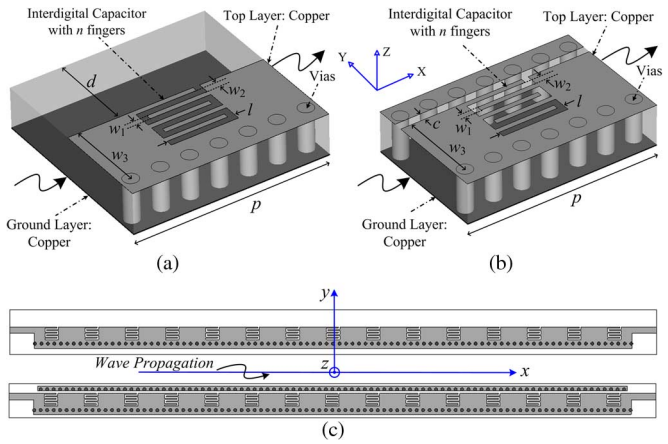

Fig. 2. Configuration of the proposed CRLH HMSIW leaky-wave structures (a) initial unit cell, (b) modified unit cell with a folded ground, and (c) overall HMSIW leaky-wave antenna prototypes.

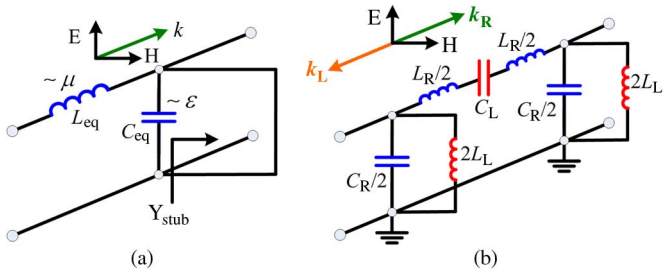

Fig. 3. Equivalent circuit models for (a) conventional SIW and HMSIW TL unit cells and (b) CRLH SIW and HMSIW leaky-wave unit cells as shown in Fig. 1(a) and Fig. 2(a).

backfire-to-endfire beam- scanning performance is confirmed by comparing the radiation patterns at different frequencies. Finally, a conclusion is drawn in Section VI.

II. Configurations

A leaky-wave antenna is a radiating transmission line structure, either in uniform or periodic configurations. In this section, the proposed leaky-wave transmission lines will be described. All the prototypes are built on the normally used substrate of Rogers 5880 with a permittivity of 2.2, a loss tangent of 0.001 and a thickness of 0.508 mm. The vias used in the models share a common diameter of 0.8 mm and a center-to-center spacing around 1.45 mm.

A. CRLH SIW Leaky-Wave Structures

Fig. 1(a) and (b) show the configurations of the one period CRLH SIW element, while the prototype of the whole transmission line with its orientation in the coordinate systems is illustrated in Fig. 1(c). For the first resonator shown in Fig. 1(a), the slot is etched on the top surface and it is grounded by a solid metallic plane. For the second resonator shown in Fig. 1(b), both the top surface and the ground are incorporated with interdigital slots with a period distance of p. The slots also provide the radiation. As indicated in Fig. 1(c) the radiation angle of the main beam is straightforwardly determined by

$$\theta(\omega) = \sin^{-1}\left[\frac{\beta(\omega)}{k_0}\right] \tag{1}$$

which shows that a full space scanning ($-90°$ to $90°$) can be achieved if $\beta(\omega)$ varies throughout the range $(-k_0, k_0)$.

B. CRLH HMSIW Leaky-Wave Structures

Fig. 2(a) and (b) show the configurations of the one period CRLH HMSIW element, while their overall transmission line structures with 15 unit cells are depicted in Fig. 2(c). For the conventional HMSIW, because of the large width-to-height ratio and the metallic via array, only the quasi-$\mathrm{TE}_{p-0.5,0}$ ($p = 1, 2\ldots$) modes can propagate in the waveguide [15]. Here the slots are embedded on the waveguide surface, leading to a CRLH HMSIW TL structure. Under this configuration wave can propagate and radiate both below and above the cutoff frequency of HMSIW while still keeping the half mode field distribution. For the second unit cell shown in Fig. 2(b), another via-wall covered by a strip on the top is placed beside the open boundary of the HMSIW. This via-wall is used to reduce the energy leakage from the open boundary. It can be viewed as a folded ground which can miniaturize the transverse size of the HMSIW, as well as restrict the radiation to go to the broadside. These leaky-wave TLs shown in Fig. 2(c) can be easily mounted on the metal surface.

III. Model Analysis and Dispersion Relation

A CRLH TL is an artificial TL structure constituted by the repetition of series capacitance and shunt inductance into a host conventional TL medium exhibiting a left-handed (LH) band at low frequencies and a right-handed (RH) band at higher frequencies. Fig. 3(a) presents the equivalent circuit model for the original SIW or HMSIW unit cell without the slots, which is similar to the traditional rectangular waveguide. The top metal

surface and the ground are modeled as a two-wire TL with distributed series inductance and distributed shunt capacitance, which are associated with the permeability and permittivity of the substrate, respectively. It is noted that the vias, as a short-circuited stub, provide the shunt inductance. Compared with the circuit model of the CRLH structures, only the series capacitance is absent and needs to be added. Fig. 3(b) depicts the circuit model of the proposed CRLH unit cells shown in Fig. 1(a), which are symmetrical. The interdigital capacitor has been introduced into the model as $C_{\rm L}$ in the center to obtain a CRLH behavior. $L_{\rm L}$ represents the inductance generated by the via-wall. They make the LH contribution. The RH contribution comes from the distributed shunt capacitance $C_{\rm R}$ and the distributed series inductance $L_{\rm R}$. Note that the series slot also plays the role of a radiating element for the leaky-wave antenna. Increasing the width and the length of the slots will make the radiation more efficient. Also bear in mind that increasing the slot width leads to a decrease of $C_{\rm L}$ while increasing the slot length results in an increase of $C_{\rm L}$. Thus enhancing the radiation does not conflict with achieving a balanced case.

The dispersion diagrams for the proposed four unit cells are then investigated in detail by using Ansoft's High Frequency Structure Simulator (HFSS) software package. Usually two approaches are adopted to calculate the dispersion curve for a single unit cell. One is obtained based on the S-parameters from driven mode simulation [34], [35]. The other one is based on the Eigen-mode simulation by applying periodic boundary conditions [35]. The Eigen-mode simulation method is more accurate but time-consuming. To give a comparison, Fig. 4(a) plots the dispersion curves of a balanced CRLH SIW unit cell using both of the two approaches. A good agreement is obtained. It is also observed from the Eigen-mode simulation that a very small bandgap (0.1 GHz) actually exists between the LH and RH regions. Fig. 4(b) presents the dispersion diagram and *Bloch* impedance obtained from driven mode simulation for a balanced CRLH SIW double-side radiating unit cell. The dispersion curves for an unbalanced CRLH HMSIW unit cell and an unbalanced modified CRLH HMSIW unit cell are shown in Fig. 4(c). The main parameter values for these unit cells are shown in the caption. In all these cases the dispersion curve traverses four distinct regions as frequency increases, named LH-guidance, LH-radiation, RH-radiation and RH-guidance here, where the radiation regions are characterized by a phase velocity larger than the speed of light (airline). For the unbalanced case shown in Fig. 4(b), a bandgap region is generated between the LH and RH regions. By moving the LH region far below the waveguide cutoff, miniaturization can be obtained. In Fig. 4(a) it is seen that a balanced case is almost achieved with the balancing point located at about 10 GHz, which ensures a seamless transition from the LH to the RH band. It happens when the series resonance frequency and shunt resonance frequency are equal, or

$$L_{\rm R} \times C_{\rm L} = L_{\rm L} \times C_{\rm R} \tag{2}$$

Under this condition the dispersion relation splits into additive positive linear RH and negative hyperbolic LH terms [16]

$$\beta(\omega) = \beta_{\rm RH} + \beta_{\rm LH} = \frac{\omega}{p}\left(\sqrt{L_{\rm R}C_{\rm R}} - \frac{1}{\omega^2\sqrt{L_{\rm L}C_{\rm L}}}\right). \tag{3}$$

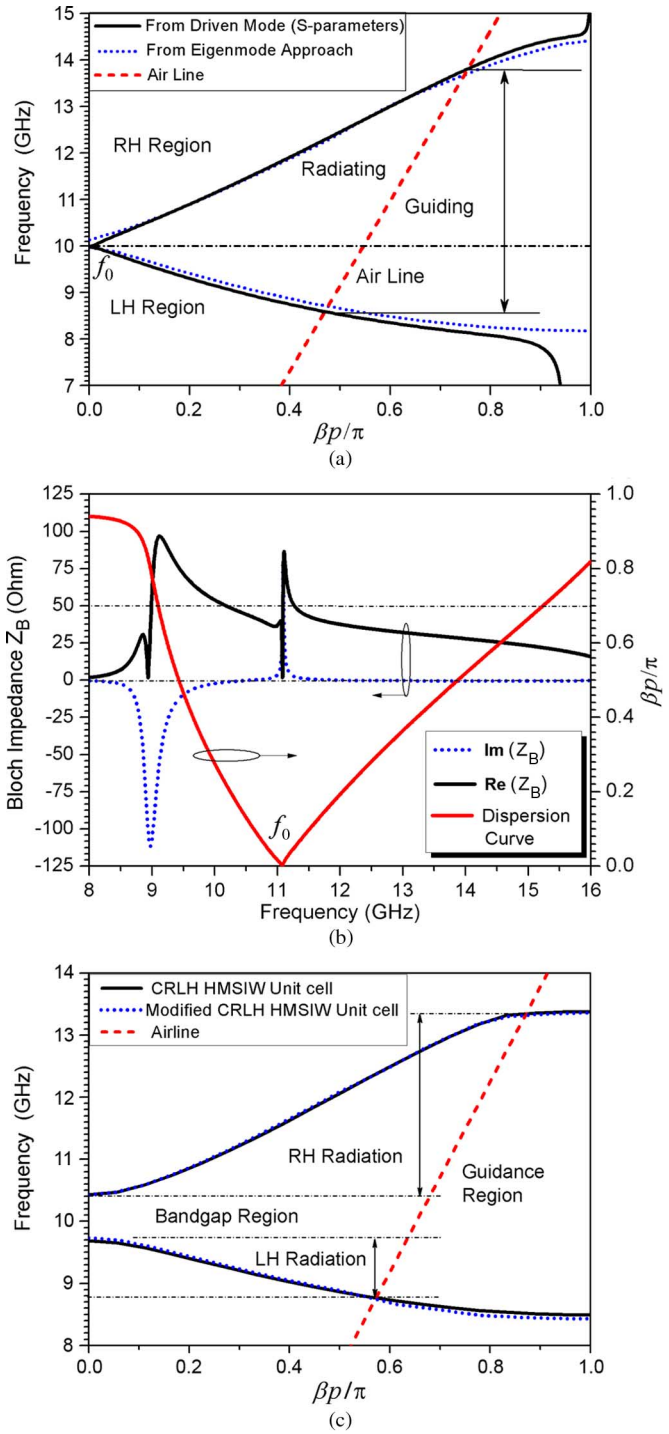

Fig. 4. (a) Dispersion diagram calculated from driven mode and Eigen- mode simulations for the single-side CRLH SIW unit cell shown in Fig. 1(a), the parameter values are: $w_1 = 0.33$ mm, $w_2 = 0.45$ mm, $w_3 = 9.2$ mm, $n = 9$, $p = 8.2$ mm, $l = 3.3$ mm; (b) dispersion curve and *Bloch* impedance obtained using driven mode simulation for the double-side CRLH SIW unit cell shown in Fig. 1(b), the parameter values are: $w_1 = 0.32$ mm, $w_2 = 0.33$ mm, $w_3 = 8.6$ mm, $n = 9, p = 7.45$ mm, $l = 2.6$ mm; (c) dispersion curve using Eigen-mode simulation for the CRLH HMSIW unit cell and modified CRLH HMSIW unit cell shown in Fig. 2, the parameter values are: $w_1 = 0.27$ mm, $w_2 = 0.36$ mm, $w_3 = 4.1$ mm, $n = 5, p = 9.8$ mm, $l = 3.3$ mm, $d = 4.4$ mm $c = 0.6$ mm.

where p is the length of the unit cell. This expression exhibits a null at the frequency

$$f_0|_{\beta=0} = \frac{1}{2\pi\sqrt{L_{\rm R}C_{\rm L}}} = \frac{1}{2\pi\sqrt{L_{\rm L}C_{\rm R}}} \tag{4}$$

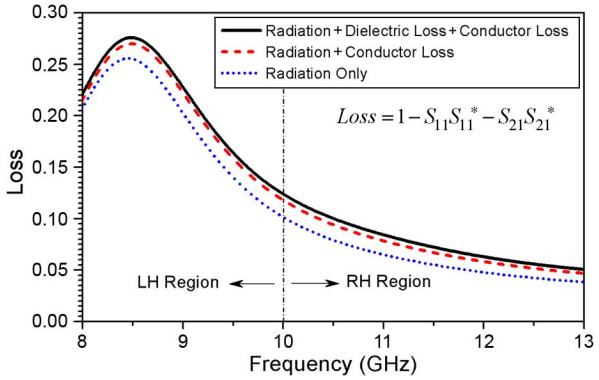

Fig. 5. Calculated different losses for the single-side CRLH SIW unit cell described in Fig. 4(a).

which is the transition frequency shown in Fig. 4(a). It should be noted that at this frequency group velocity is nonzero despite the infinite phase velocity, which allows leaky-wave broadside radiation.

For a specified antenna design requirement, the width of the waveguide can be first chosen to approximately locate the RH region. Then we determine the size of the interdigital slot to roughly get the LH region. Due to the difficulty in extracting those lumped values (L_{L}, C_{L}, L_{R} and C_{R}), some numerical optimization is necessary to obtain a seamless transition for a balanced case or a required bandgap for an unbalanced case. It is also noted that the impedance matching should also be taken into account during the design process. However this matching can be designed in the last step using a taper line at the two ends of a leaky-wave antenna [2]. As the *Bloch* impedance shown in Fig. 4(b), the average value (real part) from 9.5 GHz to 13 GHz is around 36 Ohm, which can be easily matched to 50 Ohm using a taper line. However for the HMSIW type the average *Bloch* impedance is close to 50 Ohm therefore no taper line is used. The different losses for the unit cell are also an important issue. Fig. 5 presents a loss analysis for the single-side CRLH SIW unit cell. It is seen that compared with the radiation, the other losses are not very significant. By a similar analysis it is found that both the dielectric loss and conductor loss for the HMSIW case are much smaller compared with the CRLH SIW unit cell, which is due to the weaker resonating field because of its one open boundary [15].

Based on these unit cells discussed above, four CRLH leaky-wave antennas are designed and fabricated, which are operated at the X-band, including two balanced SIW designs as shown in Section IV and two unbalanced HMSIW designs which will be discussed in Section V.

IV. CRLH SIW Leaky-Wave Antennas

Here two CRLH SIW leaky-wave antennas are designed and fabricated using the substrate of Rogers 5880 with a thickness of 0.508 mm and a relative permittivity of 2.2. The first leaky-wave antenna is one-side radiating while the second one is a double-side radiating antenna which is realized by etching slots on both the top surface and the ground as indicated by Fig. 1. Fig. 6 shows the photograph of the fabricated antennas. The full-wave simulation is performed using the CST Microwave

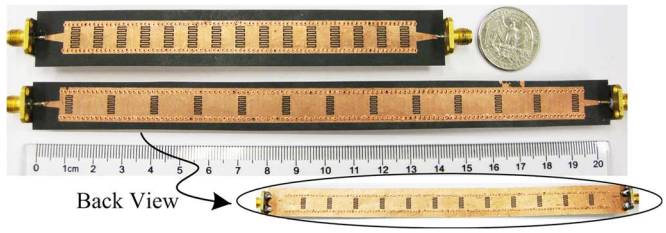

Fig. 6. Photograph of the two fabricated CRLH SIW leaky-wave antennas.

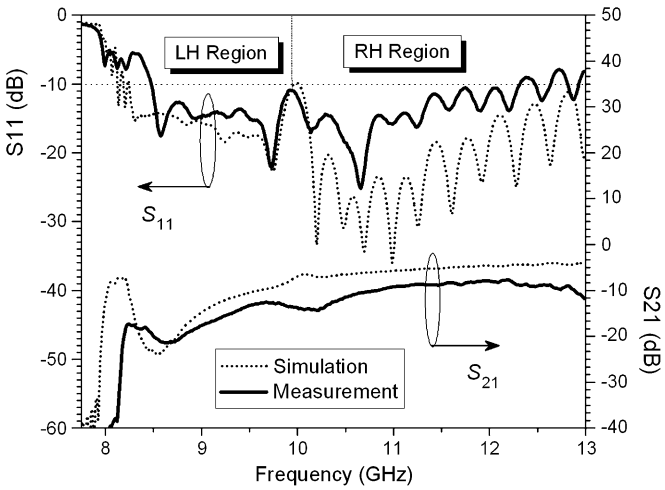

Fig. 7. Measured and simulated S-Parameters for the one-side radiating CRLH SIW leaky-wave antenna.

studio. Their performance will be discussed in the following part of this section.

A. One-Side Radiating Leaky-Wave Antenna

The first antenna has 15 identical elementary cells. The dispersion relation and parameter values for the unit cell have already been presented in Fig. 4 of the above section. Fig. 7 shows the measured and simulated S-parameters of this leaky-wave antenna, which are in good agreement. A satisfactory return loss above 10 dB in the band of interest (from 8.5 GHz to more than 12 GHz) is achieved. The insertion loss is almost below -10 dB, which indicates good leakage radiation. The curve also shows that in the LH region, the radiation is more effective compared with that in the RH region. The discrepancy of S_{21} between the simulation and measurement is due to the increase of reflection, the loss from the SMA connectors and probably the increased conductor loss.

Its CRLH behavior is verified by the field distribution along the structure as shown in Fig. 8. In the LH band, the phase and group velocities are anti-parallel, and the wave propagation is backward. At the transition frequency, infinite guided wavelength is observed and there are no field variations. However the group velocity is nonzero ($v_g = \partial\omega/\partial\beta \neq 0$), thus the wave is still propagating and radiating. In the RH band, the phase and group velocities are parallel, and the wave propagation is forward. Also note that when the frequency is close to the balanced frequency as shown in Fig. 8(a), the guided wavelength is larger corresponding to less field variations compared with the case shown in Fig. 8(c).

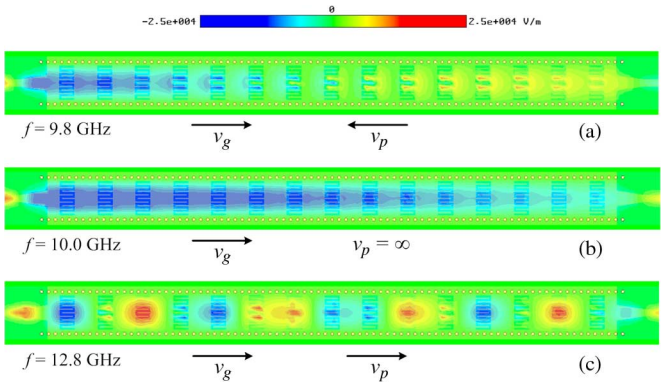

Fig. 8. Electric field distribution at different frequencies for the CRLH SIW leaky-wave antenna. (a) 9.8 GHz in LH region, (b) 10.0 GHz at the transition point, and (c) 12.8 GHz in the RH region.

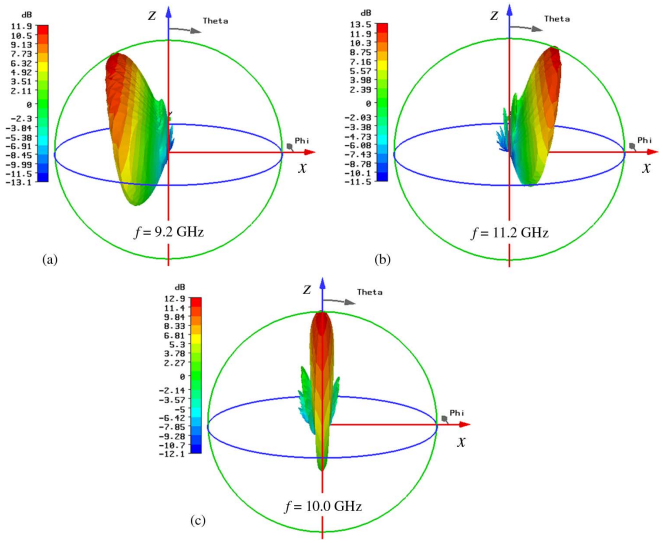

Fig. 9. Simulated 3-D radiation patterns at different frequencies for the CRLH SIW leaky-wave antenna. (a) 9.2 GHz in LH region, (b) 11.2 GHz in the RH region, and (c) 10.0 GHz at the transition point.

Fig. 9 shows the simulated 3-D radiation patterns. It is seen that, when the frequency is increased, the main beam moves from the backfire towards the endfire direction. At the transition frequency, the radiation goes exactly to the broadside.

Fig. 10 and Fig. 11 show the normalized radiation patterns measured at different frequencies. The E-plane radiation patterns at 8.6 GHz and 9.3 GHz in the LH region are given by Fig. 10(a). We find that at 8.6 GHz the beam angle θ is about $-70°$, very close to backfire. Fig. 10(b) presents the E-plane radiation patterns in the RH region. It is found that at 12.8 GHz the beam angle θ switches to approximately 60°. Fig. 11 displays the measured broadside radiation patterns for both the co-polarization and cross-polarization in the E-plane and H-plane. We see that the cross-polarization level is very low and is almost negligible.

Fig. 12 shows antenna gain response. The simulated radiation efficiency is also plotted in this figure. We find there is a discrepancy around 1.8 dB between the simulated and measured gains. The backfire-to-endfire beam-steering capability by the way of

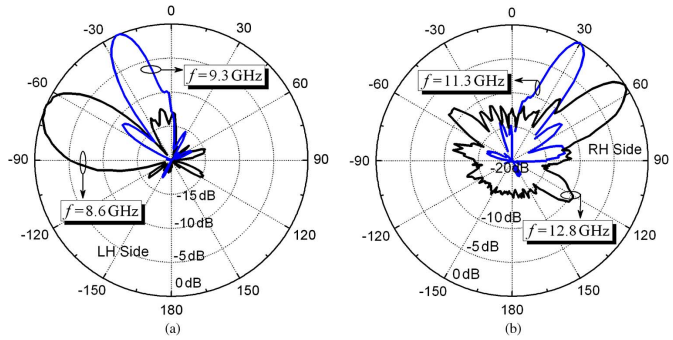

Fig. 10. Measured radiation patterns of the single-side SIW leaky-wave antenna (a) E-plane ($x-z$ plane) in the LH region, (b) E-plane ($x-z$ plane) in the RH region.

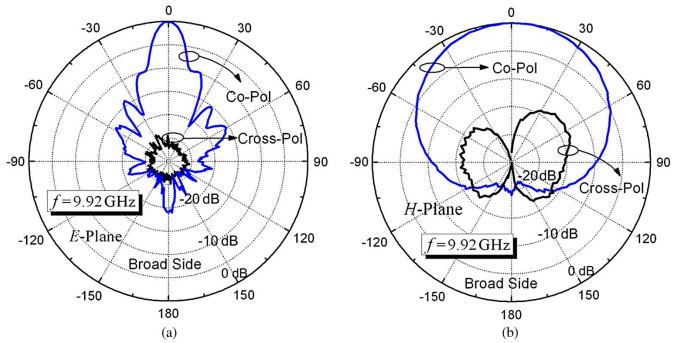

Fig. 11. Measured radiation patterns at the balanced frequency for the single-side SIW leaky-wave antenna (a) in E-plane ($x-z$ plane), (b) in H-plane ($y-z$ plane).

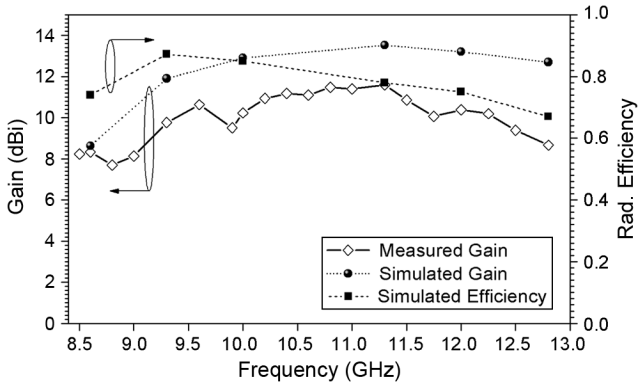

Fig. 12. Gain and the simulated radiation efficiency of the single-side CRLH SIW leaky-wave antenna.

frequency scanning is confirmed with a maximum gain of approximately 10.8 dBi and an average efficiency of 82% for this antenna.

B. Double-Side Radiating Leaky-Wave Antenna

The double-side radiating leaky-wave antenna has a total number of 25 interdigital slots etched on the top surface and the ground of the SIW. The simulated and measured transmission response is shown in Fig. 13. Still a balanced case is realized in order to obtain a continuous beam-steering function. The observed S_{11} and S_{21} are quite low indicating a good matching

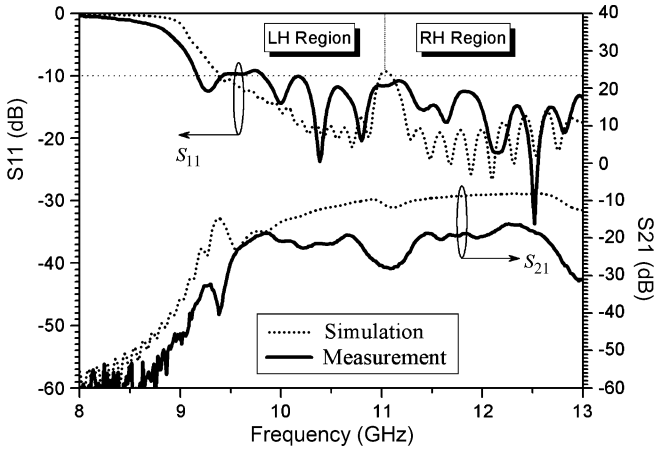

Fig. 13. Measured S-Parameters of the double-side radiating CRLH SIW leaky-wave antenna. Parameter values are shown in Fig. 4.

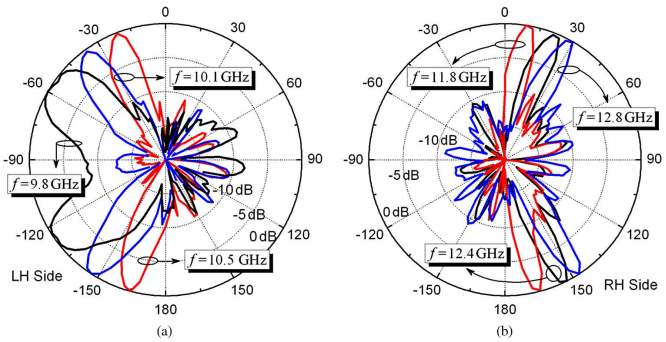

Fig. 14. Measured radiation patterns of the double-side radiating CRLH SIW leaky-wave antenna (a) E-plane ($x-z$ plane) in the LH region, (b) E-plane ($x-z$ plane) in the RH region.

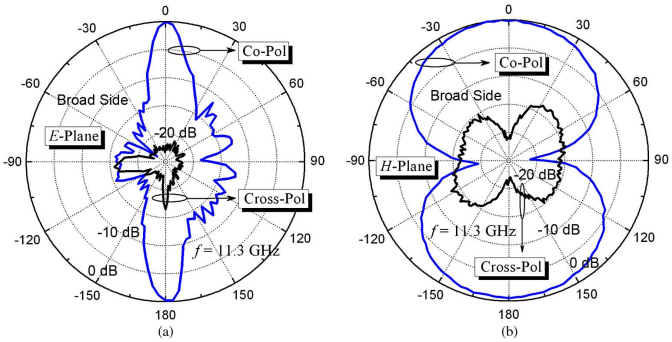

Fig. 15. Measured radiation patterns at the balanced frequency for the double-side SIW leaky-wave antenna (a) in E-plane ($x-z$ plane), (b) in H-plane ($y-z$ plane).

and a good radiation performance. The connector loss, increased reflection and conductor loss are also responsible for the visible discrepancy of S_{21}.

Fig. 14 shows the measured E-plane radiation patterns in the LH and RH regions, respectively. Fig. 15 gives the radiation patterns for the co-polarization and cross- polarization at the transition frequency in both the E-plane and H-plane. The E-plane patterns are similar to the inline element arrays while for the latter beam-steering is usually achieved by phase control which requires a complicated feeding network. This antenna has quasi-

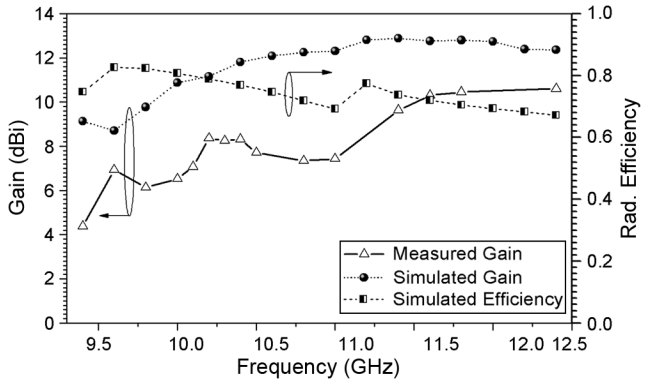

Fig. 16. Antenna gain and the simulated radiation efficiency of the double-side radiating CRLH SIW leaky-wave antenna.

omnidirectional radiation in H-plane with a low cross-polarization level. We also find that the main beam for this antenna is sharper compared with the first antenna. This is due to the reason that the distance between the unit cells on one side is increased for this second antenna, which results in the decrease of the beamwidth according to the array theory. This also explains that the beamwidth in the LH region (at low frequencies) is larger than that in the RH region (at high frequencies corresponding to a smaller wavelength). Fig. 16 shows the measured and simulated antenna gains, as well as the simulated radiation efficiency. Its double-side radiating nature would decrease the antenna gain by 3 dB compared with the first antenna in theory. However, this antenna has a larger aperture size with respect to the single-side radiating antenna. Therefore, the observed gain difference between in simulation is only around 1 dB. The measured gain is 2–3 dB lower than that from the simulation.

C. Discussion on Antenna Losses

In both of the above two cases, the measured gain and S_{21} are lower than those obtained from simulation using CST microwave studio. There are several reasons: 1) The conductor loss and dielectric loss in the measurement should be higher than that in the simulation, especially the conductor loss. The antennas were fabricated by us based on chemical etching and the observed conductor surface is not very smooth which would lead to an increase on the conductor loss; 2) The loss from the SMA connectors is not included in the simulation; 3) The measured gain takes the reflection (S_{11}) and terminated power (S_{21}) in to account; 4) We found that our chamber is not big enough. In the measurement our antennas are located close to the far field region but not exactly in the far field area, especially for the double-side antenna. This would lead to some inaccuracy for the gain measurement. These factors could all cause the decrease of the measured antenna gain.

V. CRLH HMSIW Leaky-Wave Antennas

Fig. 17 shows the photograph of the two CRLH HMSIW leaky-wave antennas. They are fabricated using the same substrate at the High Frequency Center of the Electrical Engineering Department of UCLA. They have the same dimensions except that an extra via-wall is placed near the open side for the

Fig. 17. Photograph of the two fabricated CRLH HMSIW leaky-wave antennas.

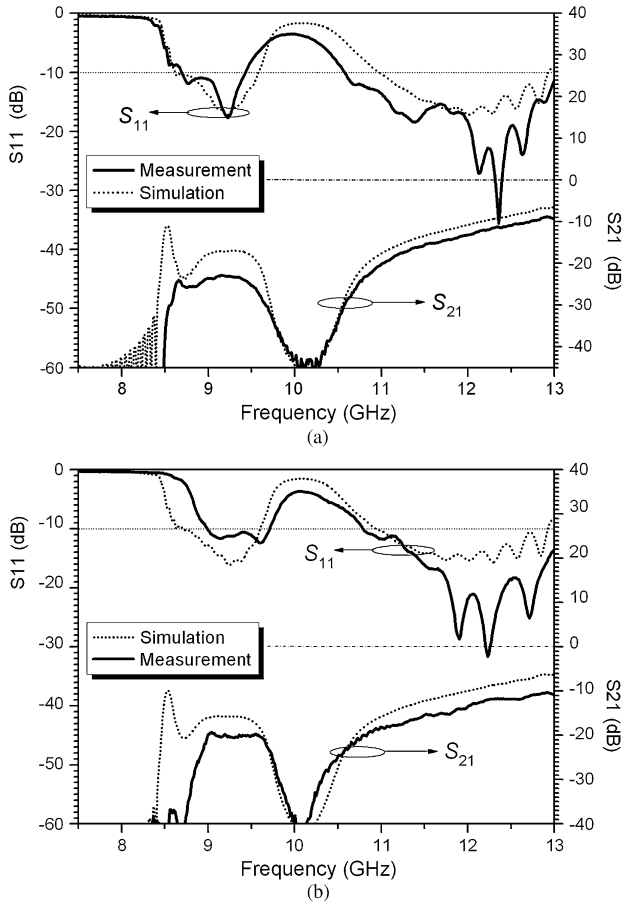

Fig. 18. Measured and simulated S-Parameters for the (a) CRLH HMSIW leaky-wave antenna and (b) Modified HMSIW leaky-wave antenna. The dimensions for the unit cells are shown in Fig. 4.

second antenna (see the modified unit-cell shown in Fig. 2(b)), which can be viewed as a folded ground and leads to a miniaturization on the transverse size. This via-wall can also reduce the wave leakage from the open boundary, thus improving the gain.

Fig. 18 shows the simulated and measured transmission responses of the two leaky-wave antennas. They are unbalanced and the dispersion diagrams for the unit cells are shown in Fig. 4(c). A bandgap region is observed in both the simulation and the measurement for these two antennas. It is important to bear in mind that by changing the slot size and the position of the vias we can easily control the position of the LH band. Balanced condition can also be obtained by some optimization as shown in [21].

Fig. 19 shows the measured radiation patterns for the first CRLH HMSIW antenna, while Fig. 20 plots the measured

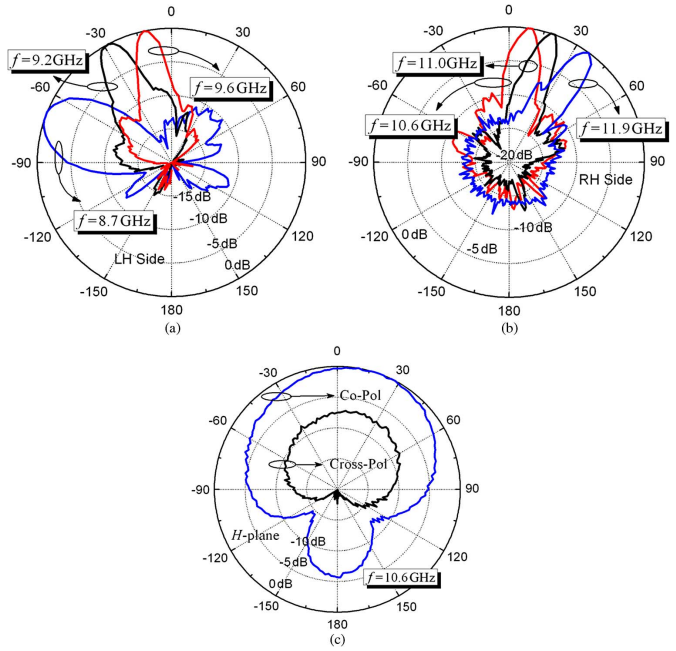

Fig. 19. Measured radiation patterns of the initial CRLH HMSIW leaky-wave antenna (a) E-plane ($x-z$ plane) in the LH region, (b) E-plane ($x-z$ plane) in the RH region, and (c) H-plane ($y-z$ plane) at 10.6 GHz.

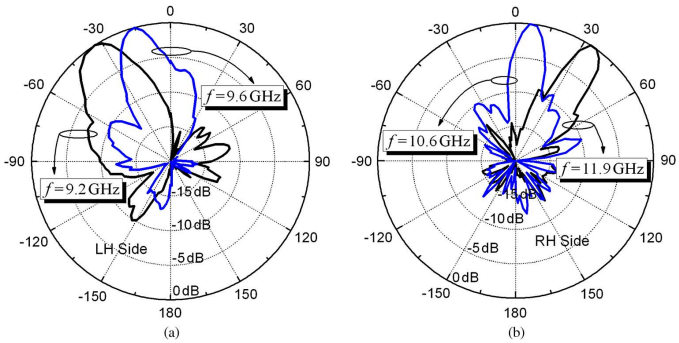

Fig. 20. Measured E-plane ($x-z$ plane) radiation patterns of the modified CRLH HMSIW leaky-wave antenna (a) in LH region and (b) in RH region.

E-plane patterns for the second CRLH HMSIW leaky-wave antenna. Beam scanning capability in E-plane for these two antennas is clearly observed. Since this is an unbalanced case and there is no balanced point which gives broadside radiation, it is difficult to obtain the H-plane radiation patterns which are observed in the $y-z$ plane. We still give the H-plane pattern measured at 10.6 GHz for the first antenna. It is noted that this measured pattern does not corresponds to the maximum value as indicated by the E-plane pattern shown in Fig. 19(b). The cross-polarization level is slightly higher compared with the CRLH SIW antennas, which is mainly due to the edge radiation caused by the open boundary.

Fig. 21 shows the simulated and measured gains, as well as the radiation efficiencies for these two antennas. It is noted that the average radiation efficiency for HMSIW antennas is around 87%, which is higher than that of the CRLH SIW leaky-wave antennas. This is because the HMSIW antennas have less conductor and dielectric losses. Especially at low frequencies, they are less lossy than the SIW [15]. A gain decrease around 2 dB

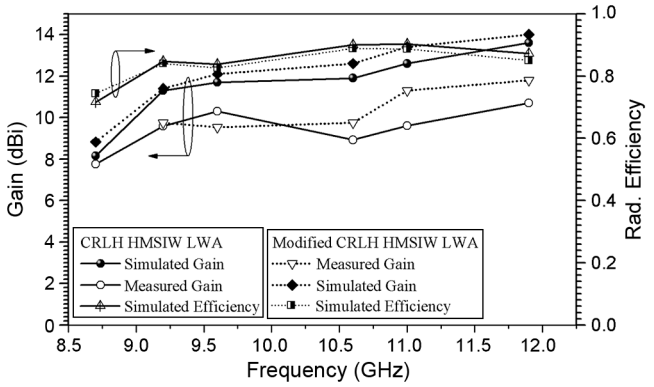

Fig. 21. Measured and simulated antenna gains of the two CRLH HMSIW leaky-wave antennas.

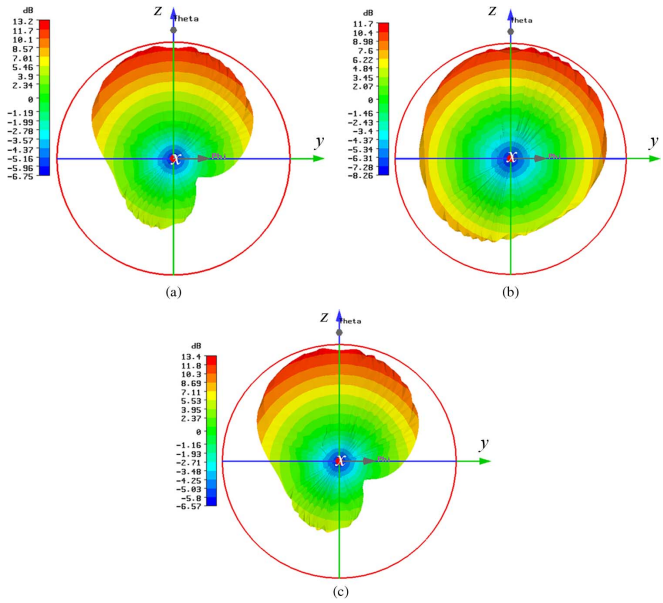

Fig. 22. Simulated radiation patterns in terms of gain at 11 GHz for the CRLH HMSIW antennas with varied configurations. (a) Initial design with the ground extension $d = 4.4$ mm, (b) initial design with the ground extension $d = 1.0$ mm, and (c) modified design with $c = 0.4$ mm.

is also observed in the measurement compared with the simulation. We also find that the gain for the second antenna with the modified structure is a little larger than the gain of the first one, although the second antenna has a smaller ground. To explain this difference, Fig. 22 plots the simulated patterns in $y-z$ plane viewed towards $-x$ direction with varied ground conditions. It is found that when the ground extension from the open boundary of HMSIW is small (c is small), the antenna has a low gain as the case shown in Fig. 22(b). However, when the extended ground is larger (c is large), the gain is increased as shown in Fig. 22(a), approaching the gain of the antenna with a folded ground as shown in Fig. 22(c).

Fig. 23 shows a parametric study about the peak gain for the antennas with different ground configurations. It is observed that if the ground extension at the open side of the HMSIW antenna is very small, the edge leakage is substantial resulting in a small gain. To reduce this undesired radiation a large ground is required. However, we can use the modified design to minimize

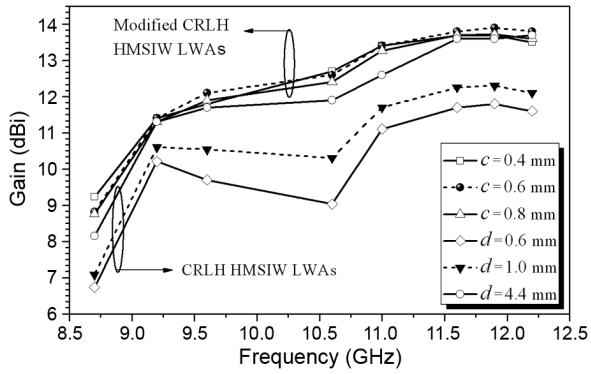

Fig. 23. Simulated antenna gains for the two CRLH HMSIW leaky-wave antennas with varied ground configurations.

the influence of the ground plane. And it is observed that the gain of the modified CRLH HMSIW antenna is not very sensitive to the distance between the via-wall and the open edge.

VI. Conclusion

A detailed investigation on a family of CRLH SIW and HMSIW leaky-wave antennas is presented in this study. Four antennas with different radiation characteristics are developed. Their circuit models are analyzed. Their dispersion relation and radiation mechanism are discussed. Their full space beam-scanning performance is confirmed by simulation and measurement. The effect of the ground for the HMSIW leaky-wave antenna is discussed and a miniaturization technique is proposed. Antenna transmission response, radiation patterns, gain and efficiency are all provided, giving designers with in-depth understanding and some useful design information. These antennas exhibit advantages in their low fabrication complexity, full space beam-scanning capability, low profile, low cost, and easy integration with other planar circuits. They are promising antenna candidates for integrated microwave and millimeter wave systems.

References

[1] J. Hirokawa and M. Ando, "Single-layer feed waveguide consisting of posts for plane TEM wave excitation in parallel plates," *IEEE Trans. Antennas Propag.*, vol. 46, no. 5, pp. 625–630, May 1998.

[2] D. Deslandes and K. Wu, "Integrated microstrip and rectangular waveguide in planar form," *IEEE Microw. Wireless Compon. Lett.*, vol. 11, no. 2, pp. 68–70, Feb. 2001.

[3] Y. Huang and K. L. Wu, "A broad-band LTCC integrated transition of laminated waveguide to air-filled waveguide for millimeter-wave applications," *IEEE Trans. Microw. Theory Tech.*, vol. 51, no. 5, pp. 1613–1617, May 2003.

[4] N. Grigoropoulos, B. Sanz-Izquierdo, and P. R. Young, "Substrate integrated folded waveguides (SIFW) and filters," *IEEE Microw. Wireless Compon. Lett.*, vol. 15, no. 12, pp. 829–831, Dec. 2005.

[5] W. Hong, B. Liu, Y. Q. Wang, Q. H. Lai, and K. Wu, "Half mode substrate integrated waveguide: A new guided wave structure for microwave and millimeter wave application," presented at the Joint 31st Int. Infrared Millimeter Waves Conf. and 14th Int. Terahertz Electron. Conf., Shanghai, China, Sep. 18–22, 2006.

[6] Y. Cassivi and K. Wu, "Low cost microwave oscillator using substrate integrated waveguide cavity," *IEEE Microw. Wireless Compon. Lett.*, vol. 13, no. 2, pp. 48–50, Feb. 2003.

[7] D. Stephens, P. R. Young, and I. D. Robertson, "W-band substrate integrated waveguide slot antenna," *Electron. Lett.*, vol. 41, no. 4, pp. 165–167, Feb. 2005.

[8] S. Park, Y. Okajima, J. Hirokawa, and M. Ando, "A slotted post-wall waveguide array with interdigital structure for 45/SPL deg/ linear and dual polarization," *IEEE Trans. Antennas Propag.*, vol. 53, no. 9, pp. 2865–2871, Sep. 2005.

[9] J. H. Lee, N. Kidera, G. DeJean, S. Pinel, J. Laskar, and M. Tentzeris, "A v-band front-end with 3D integrated cavity filters/duplexers and antenna in LTCC technologies," *IEEE Trans. Microw. Theory Tech.*, vol. 54, no. 7, pp. 2925–2936, Jul. 2006.

[10] B. Liu, W. Hong, Y. Q. Wang, Q. H. Lai, and K. Wu, "Half mode substrate integrated waveguide (HMSIW) 3 db coupler," *IEEE Microw. Wireless Compon. Lett.*, vol. 17, no. 1, pp. 22–24, Jan. 2007.

[11] Y. Cheng, W. Hong, and K. Wu, "Half mode substrate integrated waveguide (HMSIW) directional filter," *IEEE Microw. Wireless Compon. Lett.*, vol. 17, no. 7, pp. 504–506, Jul. 2007.

[12] X. P. Chen, K. Wu, and Z. L. Li, "Dual-band and triple-band substrate integrated waveguide filters with chebyshev and quasi-elliptic responses," *IEEE Trans. Microw. Theory Tech.*, vol. 55, no. 12, pp. 2569–2577, Dec. 2007.

[13] T. M. Shen, C. F. Chen, T. Y. Huang, and R. B. Wu, "Design of vertically stacked waveguide filters in LTCC," *IEEE Trans. Microw. Theory Tech.*, vol. 55, no. 8, pp. 1771–1779, Aug. 2008.

[14] W. Che, L. Geng, K. Deng, and Y. L. Chow, "Analysis and experiments of compact folded substrate-integrated waveguide," *IEEE Trans. Microw. Theory Tech.*, vol. 56, no. 1, pp. 88–93, Jan. 2008.

[15] Q. H. Lai, C. Fumeaux, W. Hong, and R. Vahldieck, "Characterization of the propagation properties of the half-mode substrate integrated waveguide," *IEEE Trans. Microw. Theory Tech.*, vol. 57, no. 8, pp. 1996–2004, Aug. 2009.

[16] C. Caloz and T. Itoh, *Electromagnetic Metamaterials Transmission Line Theory and Microwave Applications*. New York: Wiley-IEEE Press, 2005.

[17] G. Eleftheriades and K. Balmain, *Negative-Refraction Metamaterials Fundamental Principles and Applications*. New York: Wiley-IEEE Press, 2005.

[18] N. Engheta and R. W. Ziolkowski, *Electromagnetic Metamaterials: Physics and Engineering Explorations*. New York: Wiley-IEEE Press, 2006.

[19] H. Zhao, T. J. Cui, X. Q. Lin, and H. F. Ma, "The study of composite right/left handed structure in substrate integrated waveguide," in *Proc. Int. Symp. Biophotonics, Nanophotonics Metamaterials*, Oct. 2006, pp. 547–549.

[20] T. Cui, X. Lin, Q. Cheng, H. Ma, and X. Yang, "Experiments on evanescent-wave amplification and transmission using metamaterial structures," *Phys. Rev. B*, vol. 73, pp. 2451191–2451198, Jun. 2006.

[21] Y. Dong and T. Itoh, "Composite right/left-handed substrate integrated waveguide and half-mode substrate integrated waveguide," in *IEEE MTT-S Int. Microw. Symp. Dig.*, Boston, 2009, pp. 49–52.

[22] K. Okubo, M. Kishihara, A. Yamamoto, J. Yamakita, and I. Ohta, "New composite right/left-handed transmission line using substrate integrated waveguide and metal-patches," in *IEEE MTT-S Int. Microw. Symp. Dig.*, Boston, 2009, pp. 41–44.

[23] Y. Dong and T. Itoh, "Composite right/left-handed substrate integrated waveguide leaky-wave antennas," in *Proc. Eur. Microw. Conf.*, Rome, Italy, Sep. 2009.

[24] S. Lim, C. Caloz, and T. Itoh, "Metamaterial-based electronically controlled transmission-line structure as a novel leaky-wave antenna with tunable radiation angle and beamwidth," *IEEE Trans. Microw. Theory Tech.*, vol. 52, no. 12, pp. 2678–2690, Dec. 2004.

[25] F. C. Miranda, C. C. Penalosa, and C. Caloz, "High-gain active composite right/left-handed leaky-wave antenna," *IEEE Trans. Antennas Propag.*, vol. 54, no. 8, pp. 2292–2300, Aug. 2006.

[26] T. Ueda, N. Michishita, M. Akiyama, and T. Itoh, "Dielectric-resonator-based composite right/left-handed transmission lines and their application to leaky wave antenna," *IEEE Trans. Microwave Theory Tech.*, vol. 56, no. 10, pp. 2259–2268, Oct. 2008.

[27] T. Ikeda, K. Sakakibara, T. Matsui, N. Kikuma, and H. Hirayama, "Beam-scanning performance of leaky-wave slot-array antenna on variable stub-loaded left-handed waveguide," *IEEE Trans. Antennas Propag.*, vol. 56, no. 12, pp. 3611–3618, Dec. 2008.

[28] S. Paulotto, P. Baccarelli, F. Frezza, and D. Jackson, "Full-wave modal dispersion analysis and broadside optimization for a class of microstrip CRLH leaky-wave antennas," *IEEE Trans. Microwave Theory Tech.*, vol. 56, no. 12, pp. 2826–2837, Dec. 2008.

[29] T. Kodera and C. Caloz, "Uniform ferrite-loaded open waveguide structure with CRLH response and its application to a novel backfire-to-endfire leaky-wave antenna," *IEEE Trans. Microwave Theory Tech.*, vol. 57, no. 4, pp. 784–795, Apr. 2009.

[30] D. Deslandes and K. Wu, "Substrate integrated waveguide leaky-wave antenna: Concept and design considerations," in *Proc. Asia-Pacific Microw. Conf.*, Suzhou, China, 2005, pp. 346–349.

[31] J. Xu, W. Hong, H. Tang, Z. Kuai, and K. Wu, "Half-mode substrate integrated waveguide leaky-wave antenna for millimeter-wave applications," *IEEE Antennas Wireless Propag. Lett.*, vol. 7, pp. 85–88, 2008.

[32] Q. H. Lai, W. Hong, Z. Q. Kuai, Y. S. Zhang, and K. Wu, "Half-mode substrate integrated waveguide transverse slot array antennas," *IEEE Trans. Antennas Propag.*, vol. 57, no. 4, pp. 1064–1072, Apr. 2009.

[33] Y. Weitsch and T. Eibert, "A left-handed/right-handed leaky-wave antenna derived from slotted rectangular hollow waveguide," in *Proc. Eur. Microw. Conf.*, Munich, Germany, Oct. 2007, pp. 917–920.

[34] D. M. Pozar, "Microwave filters," in *Microwave Engineering*, 3rd ed. Hoboken, NJ: Wiley, 2005, ch. 8.

[35] *"Left-Handed Metamaterial Design Guide,"* Ansoft Corporation, 2007.

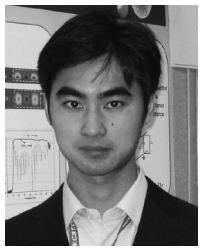

Yuandan Dong (S'09) received the B.S. and M.S. degrees from Southeast University, Nanjing, China, in 2006 and 2008, respectively. He is currently working toward the Ph.D. degree at the University of California at Los Angeles (UCLA).

From September 2005 to August 2008, he was studying at the State Key Lab. of Millimeter Waves, Southeast University. His research interests include the characterization and development of RF and microwave components, circuits, antennas and metamaterials.

Tatsuo Itoh (S'69–M'69–SM'74–F'82–LF'06) received the Ph.D. degree in electrical engineering from the University of Illinois, Urbana, in 1969.

After working for the University of Illinois, SRI, and the University of Kentucky, he joined the faculty at The University of Texas at Austin, in 1978, where he became a Professor of electrical engineering in 1981. In September 1983, he was selected to hold the Hayden Head Centennial Professorship of Engineering at The University of Texas. In January 1991, he joined the University of California, Los Angeles, as a Professor of electrical engineering and holder of the TRW Endowed Chair in Microwave and Millimeter Wave Electronics (currently Northrop Grumman Endowed Chair). He has published 375 journal papers, 775 refereed conference presentations and has written 43 books/book chapters in the area of microwaves, millimeter-waves, antennas and numerical electromagnetics. He generated 70 Ph.D. students.

Dr. Itoh is a member of the Institute of Electronics and Communication Engineers of Japan, and Commissions B and D of USNC/URSI. He received a number of awards including the IEEE Third Millennium Medal in 2000, and the IEEE MTT Distinguished Educator Award in 2000. He was elected to a member of National Academy of Engineering in 2003. He served as an Editor of the IEEE TRANSACTIONS ON MICROWAVE THEORY AND TECHNIQUES for 1983–1985. He was President of the Microwave Theory and Techniques Society in 1990. He was the Editor-in-Chief of the IEEE MICROWAVE AND GUIDED WAVE LETTERS from 1991 through 1994. He was elected as an Honorary Life Member of the MTT Society in 1994. He was the Chairman of Commission D of International URSI for 1993–1996. He serves on advisory boards and committees of a number of organizations. He served as Distinguished Microwave Lecturer on Microwave Applications of Metamaterial Structures of IEEE MTT-S for 2004–2006.